Article Category: Original Article

Genetic consequences of habitat fragmentation in a perennial plant *Trillium camschatcense* are subjected to its slow-paced life history

Yoichi Tsuzuki[1]*, Mitsuhiko P. Sato[2], Ayumi Matsuo[2], Yoshihisa Suyama[2], Masashi Ohara[1]

1. Graduate School of Environmental Science, Hokkaido University, N10W5, Sapporo, Hokkaido, 060-0810, Japan
2. Kawatabi Field Science Center, Graduate School of Agricultural Science, Tohoku University, 232-3 Yomogida, Naruko-onsen, Osaki, Miyagi, 989-6711, Japan
* corresponding author: yoichi.tsuzuki.95@gmail.com

Abstract

Many wild populations are suffering from the loss of genetic diversity caused by habitat fragmentation, while the degree of diversity loss differs among species and populations based on their life history characteristics. *Trillium camschatcense*, an understory perennial plant, has undergone intensive habitat fragmentation in the Tokachi region, Hokkaido, Japan. Although demographic deteriorations, such as reduced seed production, were already reported, genetic consequences of fragmentation have not been studied with reference to its life history. Here, we examined how life history events (e.g., growth and reproduction) and the stochasticity therein influence genetic diversity in two (each large and small) fragmented *T. camschatcense* populations. Genetic diversity was evaluated using genome-wide 2,008 single nucleotide polymorphisms (SNPs). In the small population, genetic diversity of newly germinated seedlings was significantly lower than that of matured life history stages, and effective number of breeders (N_b) was smaller than that of the large population. Simulations using a matrix population model showed that the diversity loss at seedlings is caused by genetic drift during reproduction, which was intensified by smaller N_b. Besides, simulations using randomly perturbed transition matrices suggested that stasis at juvenile stages, which is a common characteristics of *T. camschatcense*, maintains genetic diversity by buffering stochastic decrease, possibly contributing to population viability. While previous studies showed the importance to facilitate reproduction and recruitment for demographic recovery, this study highlighted the crucial roles of juvenile survival in terms of genetic diversity for the conservation of fragmented *T. camschatcense* populations in the Tokachi region.

Keywords

demographic genetic structure, demographic stochasticity, genetic drift, matrix population model, stasis

1 Introduction

Anthropogenic land-use changes have been causing habitat loss and fragmentation worldwide, resulting in local extinction of many plant populations (Aguilar et al., 2018; Krauss et al., 2010). Small fragmented populations suffer from demographic and environmental stochasticity, both of which accelerate population shrinkage (Lande, 1988). Besides, habitat fragmentation is predicted to decrease genetic diversity through bottleneck, genetic drift, restricted gene flow, and inbreeding (Aguilar, Quesada, Ashworth, Herrerias-Diego, & Lobo, 2008; Lowe, Boshier, Bacles, & Navarro, 2005; Young, Boyle, & Brown, 1996). Reduction in genetic diversity not only constrains the evolutionary potential (Bakker, van Rijswijk, Weissing, & Bijlsma, 2010; Ramsayer, Kaltz, & Hochberg, 2012), but could also suppress individual fitness and population growth (Reed & Frankham, 2003; Williams, 2001), thus threatening population viability. Hence, it is necessary to evaluate and mitigate the genetic impacts of habitat fragmentation on remnant populations.

Although many studies indicate that population shrinkage is a major driver of genetic diversity loss (Leimu, Mutikainen, Koricheva, & Fischer, 2006; Lowe et al., 2005), the susceptibility of genetic diversity to population decline differs among species and populations depending on their life history characteristics (Aguilar et al. 2008; González, Gómez-Silva, Ramírez, & Fontúrbel, 2019; Kramer, Ison, Ashley, & Howe, 2008). Life history is a lifetime trajectory of individuals from birth to death, and because genetic information is stored in individuals, genetic dynamics is fundamentally subjected to life history (Li, Kurokawa, Giaimo, & Traulsen, 2016). In perennial plants, for example, slow growth and prolonged lifespan could allow old-aged individuals to persist for many years, resulting in slow generation turnover and delayed loss of genetic

diversity (Aparicio, Hampe, Fernández-Carrillo, & Albaladejo, 2012; Martins et al., 2015). It is important, therefore, to account for life history features to successfully assess genetic impacts of habitat fragmentation.

One way to take the entire life history into account is to comparatively evaluate genetic diversity among different age or stage classes. The resultant genetic structure is referred to as demographic genetic structure (Aldrich, Hamrick, Chavarriaga, & Kochert, 1998), and can reflect genetic consequences of all life history events, such as growth and reproduction. For example, comparison between reproductive adults and newborn progenies enables us to assess how much genetic drift during reproduction decreases genetic diversity (Aguilar et al. 2008). Moreover, demographic genetic structure could reveal potential genetic changes that accompany generation turnover from mature to juvenile individuals, providing an early-warning signal of diversity loss in fragmented populations (Aldrich et al., 1998; Ally & Ritland, 2006). However, demographic genetic structure is a static and momentary data because it is usually obtained at a single time point. Evaluating the long-term genetic changes requires additional knowledge on temporal dynamics. Integrating population dynamics models, which describe temporal changes in population size based on an individual survival and reproduction, with genetic data would be an effective solution.

Trillium camschatcense is an understory perennial plant which is widely distributed in northeast Asia including Japan, Russia, and Korean Peninsula. The center of its distributional range is Hokkaido, northern Japan. Although this species was once abundant in Hokkaido, its habitats have been destroyed due to agricultural and residential land development since the late 19th century (Ohara, Toimmatsu, Takada, & Kawano, 2006). One of the most striking habitat destructions took place in the Tokachi

region (Figure 1(a)). According to the records in the early time of land development (Hokkaido Government, 1897), this region had been almost completely forested, and understory plants including *T. camschatcense* were extensively distributed. However, intensive land development which started in the 1880s resulted in many small forest fragments within an agricultural matrix (Figure 1(b)). Previous studies have shown that the fragmentation restricts both seed production and the establishment of seedlings (Tomimatsu & Ohara, 2002; Tomimatsu & Ohara, 2004). Besides, a matrix population model, which was parameterized by individual survival rates and fecundity at every life history stage, was constructed based on six years of demographic monitoring in four fragmented populations (Tomimatsu & Ohara, 2010). Despite these achievements, genetic consequences of habitat fragmentation have not been well clarified in this system, although bottleneck effect was revealed by allozyme analysis on flowering individuals (Tomimatsu & Ohara, 2003).

Here, we combined empirically estimated demographic genetic structure with the previously constructed matrix population model and assessed how habitat fragmentation interacts with life history to influence genetic diversity and its long-term temporal dynamics of *T. camschatcense* in the Tokachi region.

2 Materials and Methods

2.1 Study system

Trillium camschatcense is a long-lived understory polycarpic plant. As with many other understory perennials, this species grows slowly with limited sunlight, taking a long period of years to become sexually mature. The prolonged life cycle can be categorized

into five distinct life history stages: seed (SE), seedling (SD), one-leaf (1L), three-leaves (3L), and flowering (FL) (Figure 2). Seeds germinate after two years of dormancy and grow as seedlings for the second year. From the third year on, they continue to grow as one-leaf and subsequently as three-leaves. It is not until they store enough assimilated resources that they become flowering. Flowering individuals are long-lived and remain reproductive for years, and sometimes retrogress to three-leaves due to resource exhaustion (Ohara & Kawano, 2005).

In May 2018, we selected 24 populations differing in habitat areas. We established one to three 5 m × 5 m quadrats in each population and recorded the number of flowering individuals within the quadrats. As a result, we found a significant positive effect of the habitat size on the density of FL (Figure 3). We selected two representative populations along the correlation: FUJ (Fuji town, Obihiro city), which is one of the largest populations in the region (density of FL = 328/25 m^{-2}, habitat area = 5.87 ha), and SAK (Sakuragi town, Obihiro city), which is a small and severely fragmented population (density of FL = 104/25 m^{-2}, habitat area = 0.71 ha).

2.2 Sampling and SNP detection

In May 2019, we established one 5 m × 5 m quadrat in each population and randomly collected leaves of 16 individuals per stage within each quadrat. We used random samples from the quadrat rather than from the entire population for two reasons. Firstly, considering that seeds of *T. camschatcense* were dispersed by ants up to only a few meters (Ohara & Higashi, 1987), the genetic composition could be highly spatially structured within a population. Therefore, the larger the sampling aera is, the higher the estimated genetic diversity can be. To evaluate the role of life history independently

138 from that of sampling area, it is thus necessary to adopt a fixed spatial scale. Secondly,
139 there is a need to adjust spatial scale of genetic data to that of the matrix population
140 model parameterized by fine-scale demographic data (Tomimatsu & Ohara, 2010) for
141 the later analysis. Because it was difficult to search and collect dormant seeds from soil,
142 we omitted sampling from the seed stage (SE). Besides, considering that there was a
143 large variation in plant size within 3L stage, we divided 3L into small (3L-1) and large
144 (3L-2) stages based on leaf size (leaf length × leaf width) with threshold of 150 cm^2
145 (approximately the midpoint of the leaf size range of 3L, see Supporting Information 1).
146 As a result, 160 samples were collected in total (16 indv./stage × 5 stages (SD, 1L, 3L-1,
147 3L-2, FL) × 2 populations). The collected leaves were first stored in the refrigerator and
148 then dried using silica gel. Genomic DNA was extracted from the dried leaves following
149 the modified CTAB method (Murray & Thompson, 1980).
150 To quantify genetic diversity, we used multiplex ISSR genotyping by
151 sequencing (MIG-seq; Suyama & Matsuki, 2015). MIG-seq is one of the reduced-
152 representation DNA sequencing techniques and detects putatively neutral genome-wide
153 SNPs adjacent to microsatellite regions. We followed the method modified from
154 Suyama and Matsuki (2015) to prepare MIG-seq library. Sequencing was performed on
155 an Illumina MiSeq Sequencer (Illumina, San Diego, CA, USA) using an MiSeq Reagent
156 Kit v3 (150 cycle paired-end; Illumina). The sequence data is available at DDBJ with
157 Accession number DRA009621.
158 Primer regions, adapter sequences, and low-quality reads were removed using
159 Trimmomatic (Bolger, Lohse, & Usadel, 2014). The remaining reads were used for *de*
160 *novo* assembly. SNPs were called using Stacks ver. 2.4 (Rochette, Rivera-Colón, &
161 Catchen, 2019). Firstly, for each sample, sequenced reads were classified into groups

named “stack,” in which the number of nucleotide mismatch was two or less (M = 2). The minimum number of reads required to form a stack is set to three (m = 3). Ungrouped reads were aligned against the assembled stacks with a more permissive criterion: four nucleotide mismatches were allowed at maximum (N = 4). Stacks from different samples were then aligned with one another to create a locus if the number of nucleotide mismatch was two or less (n = 2). These parameter values are the default of Stacks *de novo* assembly. After these alignment procedures, SNPs which were successfully typed in at least 80% of all samples (r = 0.8, p = 1) were extracted with additional two criteria: minimum allele frequency must exceed 0.01 (min-maf = 0.01) and observed heterozygosity must be below or equal to 0.6 (max-obs-het = 0.6). Among the extracted SNPs, we randomly selected one SNP per locus to avoid strong linkage (write-random-snp). The resultant 2,008 SNPs were used for the following analyses.

To confirm the robustness of the results, we also called SNPs using various m, M, N, and r (m = 3, 5, 8; M = 1, 2, 3; N = M + 2; r = 0.7, 0.8, 0.9). Different m, M, and N were used with r being kept at 0.8, while different r values were used under the default m, M, and N (i.e., m = 3, M = 2, N = 4). Besides, to evaluate the influence of missing data, we excluded samples in which more than 30 % of SNPs were missing when m, M, N, and r were 3, 2, 4, and 0.8, respectively. Because these various settings yielded qualitatively similar results, we only present the results of the following parameter settings: m = 3, M = 2, N = 4, r = 0.8. The results under the other parameter values were available in Supporting Information 2.

2.3 Demographic genetic structure

Allelic richness (A_R), effective number of alleles (A_E), observed heterozygosity (H_O),

186 expected heterozygosity (H_E), gene diversity (H_S), and standardized multilocus
187 heterozygosity (sMLH), were calculated for each life history stage. Allelic richness is
188 the number of alleles adjusted by rarefaction. Effective number of alleles is the inverse
189 of the sum of squared allele frequencies and reflects not only the number but also the
190 evenness of alleles in a population. While expected and observed heterozygosity are
191 conventionally used to quantify intrapopulation diversity, gene diversity is an unbiased
192 estimator of expected heterozygosity for small sample size (Nei & Chesser, 1983).
193 Standardized multilocus heterozygosity is the proportion of heterozygous loci in an
194 individual divided by the average observed heterozygosity in the population over the
195 subset of loci successfully typed in the focal individual, and is thus measured on an
196 identical scale for all individuals (Coltman, Pilkington, Smith, & Pemberton, 1999).
197 Inbreeding coefficient (F_{IS}), which represents the level of inbreeding and is expected to
198 increase with time in isolated populations, was also estimated. All metrics except H_E
199 and sMLH were calculated with the modified function of “allelic.richness” and
200 “basic.stats” in R package “hierfstat” (Goudet, 2005), and the R code is provided in
201 Supporting Information 3. H_E and sMLH were calculated using the function “Hs” and
202 “sMLH” in R package “adegenet” and “inbreedR”, respectively (Jombart, 2008; Stoffel
203 et al., 2016).
204 Permutation test was used to evaluate whether genetic diversity (A_R, A_E, H_O,
205 H_E, H_S, and mean sMLH) became lower and inbreeding coefficients (F_{IS}) became
206 higher in more juvenile stages. For all pairs of two stages, we randomly shuffled the
207 assignment of stages to individuals without replacement and calculated the seven
208 metrics. We subtracted the diversity estimates (A_R, A_E, H_O, H_E, H_S, and mean sMLH)
209 of more juvenile stage from those of more matured stage, while subtracting F_{IS} of more

matured stage from that of more juvenile stage. The subtracted values were used as test statistics, and their null distributions were generated by repeating these procedures for 999 times. The one-sided *p*-value was obtained as the frequency of 999 simulated and one observed value greater than or equal to the observed value. *P*-values were adjusted by sequential Bonferroni method for multiple comparison. The R code used for permutation test is provided in Supporting Information 4.

2.4 Effective number of breeders

Effective number of breeders (N_b) is the counterpart of effective population size (N_e) per single reproductive season, not per generation (Waples & Teel, 1990). N_b represents the idealized number of reproductive individuals showing the same rate of genetic diversity loss from adults to offspring as the observed data. “Idealized” means that adults randomly mate and produce the same number of offspring as themselves. N_b reflects any factors involved in reproduction, such as the number of mating individuals and the per capita fecundity. Hence, the reduction in genetic diversity from flowering (FL) to seedlings (SD) during reproduction could be well evaluated by N_b.

In estimating N_b, we followed the method of Hui and Burt (2015), which estimates N_e from allele frequency data of different generations using maximum likelihood method. Here, we assumed FL and SD as two consecutive generations. This assumption is realistic, because SD is a two-year-old cohort whose parents are likely to remain in FL considering the rarity of individual turnover in the flowering stage in this species (Ohara & Kawano, 2005). We used these two “generations” to estimate N_b using the function “NB.estimator” in R package “NB” (Hui & Burt, 2015).

2.5 Model structure

We used a matrix population model to simulate the temporal dynamics of genetic diversity for FUJ and SAK populations. Matrix population models are usually used to predict discrete-time population dynamics of age- or stage-structured populations and consist of demographic rates, which are survival rates and fecundity of each age/stage class (Caswell, 2001). In *T. camschatcense*, which has five life history stages (SE, SD, 1L, 3L, and FL), annual population dynamics can be modeled as follows:

$$\begin{pmatrix} n_{SE,t+1} \\ n_{SD,t+1} \\ n_{1L,t+1} \\ n_{3L,t+1} \\ n_{FL,t+1} \end{pmatrix} = \begin{pmatrix} 0 & 0 & 0 & 0 & f \\ g_0 & 0 & 0 & 0 & 0 \\ 0 & g_1 & s_2 & 0 & 0 \\ 0 & 0 & g_2 & s_3 & r_4 \\ 0 & 0 & 0 & g_3 & s_4 \end{pmatrix} \begin{pmatrix} n_{SE,t} \\ n_{SD,t} \\ n_{1L,t} \\ n_{3L,t} \\ n_{FL,t} \end{pmatrix} \quad (1)$$

$n_{i,t}$ denotes the number of individuals in stage i in year t. Elements in the matrix include the probabilities of germination (g_0), growth (g_1, g_2, g_3), stasis (remaining in the same stage; s_2, s_3, s_4), retrogression (going backward to previous stage; r_4), and fecundity (f) per year (Figure 4). Because it is unfeasible to track the survival/death of dormant seeds in field, fecundity is usually estimated as a product with the germination rate in the next year, as in Tomimatsu and Ohara (2010). To separate f and g_0, we assumed that the g_0 was either 0.2, 0.4, 0.6, 0.8, or 1, and carried out the following analyses for each case.

We applied the matrix population model to predict temporal changes in allele frequencies. We assumed a biallelic neutral locus with alleles *A* and *a*. Since *T. camschatcense* is a diploid species, there can be three genotypes: *AA*, *Aa*, and *aa*. The transition probabilities (i.e., growth, stasis, and retrogression probabilities) and the fecundity were set to be equal among all genotypes. The number of individuals per genotype per stage can be predicted by extending the model as follows.

$$\begin{pmatrix} \boldsymbol{N}_{\mathbf{SE},t+1} \\ \boldsymbol{N}_{\mathbf{SD},t+1} \\ \boldsymbol{N}_{\mathbf{1L},t+1} \\ \boldsymbol{N}_{\mathbf{3L},t+1} \\ \boldsymbol{N}_{\mathbf{FL},t+1} \end{pmatrix} = \begin{pmatrix} \boldsymbol{O} & \boldsymbol{O} & \boldsymbol{O} & \boldsymbol{O} & \boldsymbol{F} \\ \boldsymbol{G_0} & \boldsymbol{O} & \boldsymbol{O} & \boldsymbol{O} & \boldsymbol{O} \\ \boldsymbol{O} & \boldsymbol{G_1} & \boldsymbol{S_2} & \boldsymbol{O} & \boldsymbol{O} \\ \boldsymbol{O} & \boldsymbol{O} & \boldsymbol{G_2} & \boldsymbol{S_3} & \boldsymbol{R_4} \\ \boldsymbol{O} & \boldsymbol{O} & \boldsymbol{O} & \boldsymbol{G_3} & \boldsymbol{S_4} \end{pmatrix} \begin{pmatrix} \boldsymbol{N}_{\mathbf{SE},t} \\ \boldsymbol{N}_{\mathbf{SD},t} \\ \boldsymbol{N}_{\mathbf{1L},t} \\ \boldsymbol{N}_{\mathbf{3L},t} \\ \boldsymbol{N}_{\mathbf{FL},t} \end{pmatrix} \quad (2)$$

$\boldsymbol{N_{i,t}}$ denotes the vector of the number of individuals in stage *i* in year *t*

$$\boldsymbol{N_{i,t}} = \begin{pmatrix} n_{i,AA,t} \\ n_{i,Aa,t} \\ n_{i,aa,t} \end{pmatrix} \quad (3)$$

where $n_{i,j,t}$ denotes the number of individuals of genotype *j* in stage *i* in year *t*. The summation of $\boldsymbol{N_{i,t}}$ is equal to $n_{i,t}$. The first matrix of the right side of Equation (2) consists of 3 × 3 submatrices which are shown in capital letters. $\boldsymbol{O}$ is a zero matrix, while the other submatrices except $\boldsymbol{F}$ are diagonal matrices whose diagonal elements are the small letters of themselves. For example, the submatrix $\boldsymbol{G_1}$ is given by

$$\boldsymbol{G_1} = \begin{pmatrix} g_1 & 0 & 0 \\ 0 & g_1 & 0 \\ 0 & 0 & g_1 \end{pmatrix} \quad (4)$$

and the other submatrices except $\boldsymbol{F}$ are similarly set. The use of diagonal submatrices holds because genotype of an individual never changes over the course of life history except reproduction, where gametes are shuffled. In deriving $\boldsymbol{F}$, we first defined $p_{A,t}$ and $p_{a,t}$ as allele frequencies of *A* and *a* in FL in year *t*. Under complete random mating, a given gamete will form a zygote with *A* and *a* with the probability of $p_{\mathrm{A,t}}$ and $p_{a,\mathrm{t}}$, respectively. Considering that flowering individuals of *AA* produce only gametes of *A*, their seeds can be split into *AA*, *Aa*, and *aa* at the ratio of $p_{A,t}$, $p_{a,t}$, and zero. Similarly, the proportions of *AA*, *Aa*, and *aa* among the seeds of *aa* individuals are zero, $p_{A,t}$, and $p_{a,t}$, respectively. In the case of *Aa* individuals which produce gametes of *A* and *a* in half, the genotypic composition of their seeds is the mean of that of *AA* and *aa* flowering individuals: $p_{A,t}/2$, 1/2 and $p_{a,t}/2$ for *AA*, *Aa*, and *aa*, respectively. Therefore,

275 $\boldsymbol{F}$ satisfies the following equations.

276 $$\boldsymbol{N_{\mathrm{SE},t+1}} = \boldsymbol{F}\,\boldsymbol{N_{\mathrm{FL},t}} = \begin{pmatrix} fp_{A,t} & fp_{A,t}/2 & 0 \\ fp_{a,t} & f/2 & fp_{A,t} \\ 0 & fp_{a,t}/2 & fp_{a,t} \end{pmatrix} \begin{pmatrix} n_{\mathrm{FL},AA,t} \\ n_{\mathrm{FL},Aa,t} \\ n_{\mathrm{FL},aa,t} \end{pmatrix} \quad (5)$$

277 The first to third column of $\boldsymbol{F}$ represent the composition of seeds produced by a
278 flowering individual of *AA*, *Aa*, and *aa*, respectively.

279 Since populations exponentially grow and become unrealistically large/small
280 under the model analyses, the number of individuals in each stage was scaled at each
281 timestep to remain constant. This assumption holds asymptotically in density-dependent
282 structured population dynamics, as in Ellner (1996). We carried out simulations at a
283 spatial scale of 25 m^2 by fixing $n_{\mathrm{FL},t}$ to the density of flowering individuals per 25 m^2
284 surveyed in 2018 for each population, while the number of individuals of the other
285 stages were set to be proportional to the stable stage structure, which is the leading right
286 eigenvector of the transition matrix. We multiplied the fixed number and the ratio of
287 three genotypes (i.e., *AA*, *Aa*, *aa*) calculated at each time step to yield the number of
288 individuals per stage per genotype, allowing changes in genetic composition while
289 keeping population size and stage structure constant.

290 We incorporated two stochastic processes, genetic drift and demographic
291 stochasticity, into the model. Genetic drift is the probabilistic fluctuations in offspring
292 allele frequency due to chance effect in random mating. Demographic stochasticity is
293 the random deviation from expected population dynamics due to the probabilistic nature
294 of individual survival and reproduction: whether to grow, stay, retrogress, or die is
295 determined probabilistically and independently among individuals. To compare the
296 genetic consequences between the two stochasticity, we carried out simulations under
297 four scenarios: (1) no stochasticity, (2) only genetic drift, (3) only demographic

298 stochasticity, and (4) both genetic drift and demographic stochasticity.

299 The degree of genetic drift per year depends on effective number of breeders
300 (N_b), and the allele frequencies of newborn seeds must be comparable with those of N_b
301 seeds produced by a random mating of flowering individuals. Thus, we did multinomial
302 sampling N_b times based on the expected genotype frequencies of seeds in the next year
303 (AA: $p_{A,t}^2$; Aa: $2p_{A,t}p_{a,t}$; aa: $p_{a,t}^2$) to obtain perturbed frequencies of seeds under genetic
304 drift ($\tilde{p}_{SE,AA,t+1}$, $\tilde{p}_{SE,Aa,t+1}$, $\tilde{p}_{SE,aa,t+1}$). We used N_b estimated from the empirical
305 genetic data for each population. $\boldsymbol{N}_{\mathbf{SE},t+1}$ can be calculated by the product of total
306 number of seeds (i.e., $n_{SE,t+1}$, or $f\,n_{FL,t}$, in Equation (1)) and the perturbed genotype
307 frequencies.

308 $$\boldsymbol{N}_{\mathbf{SE},t+1} = f n_{FL,t} \times \begin{pmatrix} \tilde{p}_{SE,AA,t+1} \\ \tilde{p}_{SE,Aa,t+1} \\ \tilde{p}_{SE,aa,t+1} \end{pmatrix} \quad (6)$$

309 On the other hand, the degree of demographic stochasticity corresponds to the
310 actual number of individuals, not N_b, and the smaller the number is, the more likely
311 actual transition probability deviates from expectation. We used multinomial sampling
312 in transition processes (Figure 4).

313 $$Multi\ (n_{i,j,t};\ t_{SE,i}, t_{SD,i}, t_{1L,i}, t_{3L,i}, t_{FL,i}, d_i)$$

314 $t_{SE,i}$, ..., $t_{FL,i}$ are the transition probabilities from stage i to the respective stages. d_i is the
315 mortality rate of stage i. Multinomial sampling from the above probability distribution
316 yields how individuals of genotype j in stage i in year t are split into all possible states
317 in the next year. As for reproduction, the number of seeds was taken from Poisson
318 distribution with mean equal to the value in the case without demographic stochasticity.
319 Mean of the distribution under scenario (3) and (4) can be calculated from Equation (5)

and (6), respectively. For example, $n_{\mathrm{SE},AA,t+1}$ follows the Poisson distribution bellow.

$$n_{\mathrm{SE},AA,t+1} \sim \begin{cases} Pois(f p_{A,t} n_{\mathrm{FL},AA,t} + f p_{A,t} n_{\mathrm{FL},Aa,t}/2) & \text{scenario 3} \\ Pois(f\ n_{\mathrm{FL},t}\ \tilde{p}_{SE,AA,t+1}) & \text{scenario 4} \end{cases}$$

The resultant number of individuals was then scaled to remain the same as the previous year. To make multinomial sampling applicable, the scaled number was always rounded off and adjusted to integer value.

All simulations were performed on R, and the code is provided in Supporting Information 5.

2.6 Simulation of the temporal genetic dynamics

Tomimatsu and Ohara (2010) estimated annual transition probabilities and a two-year fecundity (annual fecundity × germination rate) in four fragmented *T. camschatcense* populations in our study region from 2000 to 2006. We used the mean over the years and the populations to construct a transition matrix.

$$\begin{pmatrix} 0 & 0 & 0 & 0 & 6.197/g_0 \\ g_0 & 0 & 0 & 0 & 0 \\ 0 & 0.477 & 0.659 & 0 & 0 \\ 0 & 0 & 0 & 0.819 & 0.082 \\ 0 & 0 & 0 & 0.130 & 0.893 \end{pmatrix} \quad (7)$$

The numerator of the top-right element (6.197) is the estimated two-year fecundity, which is divided by germination rate g_0 to obtain annual fecundity. The initial ratio of the three genotypes (*AA*, *Aa*, *aa*) was set to 1:2:1 for each stage. We then simulated 200 years of temporal dynamics of expected heterozygosity for 100 times under the four scenarios as explained earlier. Average expected heterozygosity for each stage and year were calculated.

2.7 Dependence of genetic diversity on demographic rates

To estimate the dependence of genetic diversity on each life history event, we evaluated the loss of genetic diversity in situations where demographic rates (i.e., transition probabilities and fecundity, or the none-zero matrix elements in Equation (7)) were randomly perturbed. We used uniform random numbers that deviate from 0 by up to 0.1 for parameter perturbation, partly following the method of Takada and Kawai (2020). The detailed procedures can be available in Supporting Information 6. 500 random transition matrices were generated and were applied to FUJ and SAK populations as previously conducted with the original transition matrix. 200 years of temporal genetic changes were computed 100 times. Average expected heterozygosity (H_E) over the 100 iterations was calculated for each stage and year. For the total of 501 simulations (500 random transition matrices and the original transition matrix), redundancy analysis (RDA) was used to examine the relationships between H_E of the five life history stages in the 200th year and demographic rates. The five H_E were ordinated with demographic rates as constraints, and the statistical significance of the overall ordination, subsequent RDA axes, and constraint variables were tested with 999 permutations (Borcard, Gillet, & Legendre, 2011). All analyses regarding RDA were carried out using an R package "vegan" (Oksanen et al., 2019).

3. Results

3.1 Demographic genetic structure

Genetic diversity and inbreeding coefficient were estimated per stage per population (Figure 5). In FUJ (large) population, although all six diversity proxies gradually increased from seedlings (SD) to flowering (FL), there were no significant differences

among the five stages. On the other hand, in SAK (small) population, genetic diversity of SD was significantly lower than that of FL and 3L-2 for all six diversity indices (Figure 5(a)–(f)). Inbreeding coefficient was not significantly different among stages in both populations, yet it steadily decreased from SD to FL in SAK population (Figure 5(g)).

3.2 Effective number of breeders

Effective number of breeders (N_b) and its 95 percent confidence interval (C.I.) were estimated (FUJ: N_b = 25.8, C.I. = 18.9–39.1; SAK: N_b = 18.0, C.I. = 14.0–24.5). N_b of SAK population was lower than that of FUJ population. The confidence interval overlapped each other, indicating that the difference between the two populations was slight.

3.3 Demographic genetic structure under different stochasticity situations

Simulation analysis revealed 200 years of temporal dynamics of expected heterozygosity (H_E) in both populations (Figure 6). Because the results are qualitatively similar among different g_0, we here present only the results of g_0 = 1 (see Supporting Information 7 for the other g_0). Without stochasticity, there were no differences in H_E among the five stages with no temporal decline at all (Figure 6(a)). However, H_E steadily decreased over the course of time if either or both stochasticity was present (Figure 6(b)–(d)). H_E of seedlings completely tracked that of seeds with one-year delay, reflecting the double dormancy of this species. The slope of temporal decrease was much steeper in SAK population than in FUJ population. Under the presence of genetic drift, H_E became lower along the maturity gradient (from matured to juvenile stages),

and H_E of seeds and seedlings was kept lower than that of the other three stages, which was more obvious in SAK population (Figure 6(b)(d)). When only demographic stochasticity was incorporated, no apparent inter-stage differences were found (Figure 6(c)).

3.4 Dependence of genetic diversity on demographic rates

Associations between H_E of the five life history stages and demographic rates were visualized in RDA correlation triplots (Figure 7). Because we got similar results under different g_0, only the results of $g_0 = 1$ were presented (see Supporting Information 8 for the other g_0). RDA was not performed for scenario 1 because H_E always remained the same as the initial condition, hardly affected by demographic rates. In the other three scenarios, RDA axis 1 had prominent explanatory power (approximately 50–80 % of the total variance, Figure 7). In RDA triplots, the angles between H_E and demographic rates reflect their correlations, while signs of the axes are arbitrary (Borcard et al., 2011). Therefore, demographic rates that were in the same direction with the five H_E regarding RDA axis 1 likely significantly contributed to high H_E. As for scenario 2, s_2 and s_3 (stasis of 1L and 3L) had relatively strong positive correlations with H_E, while g_2 and g_3 (growth of 1L and 3L) had negative correlations (Figure 7(a)). In other words, populations with high stasis probabilities at juvenile stages maintained genetic diversity under genetic drift. In scenario 3, H_E were positively correlated with s_3 (Figure 7(b)), indicating that genetic diversity was maintained when s_3 was high under demographic stochasticity. In scenario 4, s_2, and s_3 strongly boosted H_E under both stochasticity (Figure 7(c)).

4 Discussion

4.1 Loss of genetic diversity in fragmented populations

We revealed that genetic diversity of seedlings (SD) was significantly lower than that of flowering (FL) and three-leaves (3L-2) individuals in the small SAK population (Figure 5(a)–(f)), and that N_b was slightly smaller in SAK than in FUJ population. Simulation results indicate that genetic drift causes the apparently lower expected heterozygosity of SE and SD compared to the other mature stages, especially in SAK population (Figure 6(b)). Therefore, the low diversity of SD observed in SAK population could be attributed to genetic drift at reproduction: small N_b caused a greater sampling bias in the genetic composition of seeds and seedlings. These results agree with previous studies showing that smaller populations suffer from genetic drift more strongly than larger ones (Crow & Morton, 1955; Lowe et al., 2005; Toczydlowski & Waller, 2019).

Besides, the apparent, although not significant, increase in inbreeding coefficient of SD in SAK population (Figure 5(g)) suggests that strong genetic drift in SAK population might be accompanied by the increased level of inbreeding. Inbreeding causes greater decrease in observed than in expected heterozygosity and would alter genotypic composition. This might be partly responsible for the statistical significance only detected in SAK population despite the seemingly identical decrease in some indices (e.g., allelic richness) in both populations, because permutation of individuals can readily detect differences in genotypic composition which allele-based indices such as allelic richness are less sensitive to.

In contrast to genetic drift, demographic stochasticity did not induce consistent differences in genetic diversity among the five stages (Figure 6(c)). This could be

438 because that demographic stochasticity occurs at all stages and results in parallel
439 decrease, while genetic drift acts at only reproduction and leads to imbalanced decline
440 in SE and SD.

441 It should be noted that genetic diversity of SAK (small) population was almost
442 at the same level as, or sometimes higher than, that of FUJ (large) population (Figure
443 5(a)–(f)), which might seem inconsistent with the simulation results showing that
444 genetic diversity decreases faster in SAK than in FUJ population and the previously
445 reported bottleneck effect (Tomimatsu & Ohara, 2003). Besides, inbreeding coefficient
446 was seemingly lower in SAK than in FUJ population (Figure 5(g)). It might be that
447 SAK had been much larger and had higher diversity than FUJ before fragmentation.
448 Large population could attract many pollinators (Tomimatsu & Ohara, 2002), and
449 resultant extensive pollination, together with self-incompatibility of this species in the
450 study region (Ohara, Takeda, Ohno, & Shimamoto, 1996), should have had lowered F_{IS}
451 in SAK population. Our results might have reflected these pre-fragmentation legacies
452 due to the few generations passed after fragmentation (Tomimatsu & Ohara, 2006). The
453 time elapsed since fragmentation itself might be shorter in SAK than in FUJ
454 populations. Moreover, our sampling strategy did not aim at inter-populational
455 comparison: we sampled individuals from a fine 5 m × 5 m quadrat, not from the whole
456 population, which can hardly detect bottleneck effect. Our focus is on the genetic
457 differences among stages within a population, which can be evaluated separately from
458 the differences among populations. The interpretation of the data is thus concrete
459 despite the potential historical factors listed above.
460

461 **4.2 Roles of life history events in maintaining genetic diversity**

High degree of stasis at 1L and 3L contributed to high genetic diversity under genetic drift in both populations (Figure 7(a)). As has been discussed above, genetic drift randomly perturbs genetic composition of SE and consequently SD year by year. Stasis enables individuals older in age to remain in juvenile stages and to coexist with younger ones, thereby mixing differently aged cohorts. Overlap of cohorts could offset annual randomness caused by genetic drift and thus maintain as the same level of genetic diversity in juveniles as in flowerings. This mechanism may be consistent with the storage effect, which was previously suggested by studies showing that generation overlap maintain genetic diversity under fluctuating selection pressures (Ellner, 1996; Ellner & Hairston, 1994). Our results also agree with the preceding finding that long lifespan could slow down generation turnover and thus delay diversity loss (Aparicio et al., 2012; Martins et al., 2015), because high stasis probabilities would extend lifespan.

Demographic stochasticity, the magnitude of which depends on the number of individuals (Lande, 1988), was mitigated by the increase in s_3 (Figure 7(b)). Since s_3 could promote accumulation of individuals and thus reduce demographic stochasticity at 3L, the results indicate that buffering demographic stochasticity at 3L is crucial for maintaining genetic diversity of the whole population. In polycarpic perennial forest herbs, survival of established individuals, rather than annual reproduction, usually plays a predominant role in population dynamics (Silvertown, Franco, Pisanty, & Mandoza, 1993). Because 3L constitutes large part of the survival process, its predominant contributions to the overall genetic dynamics might have been highlighted.

In the most realistic scenario where both genetic drift and demographic stochasticity occur (scenario 4), stasis at 1L and 3L maintained high genetic diversity. The high degree of stasis at juvenile stages is a common characteristic of *T.*

camschatcense (Ohara & Kawano, 2005), implying that the two examined populations might maintain genetic diversity and population viability unless its life history is not severely altered. In general, habitat fragmentation adversely affects survival and growth of plant seedlings (Aguilar et al., 2019). It would be necessary to examine if fragmentation also alters survival and growth of juveniles to evaluate the risk of genetic diversity loss.

5. Conclusion

The present study examined how life history events and the stochasticity therein interact with habitat fragmentation and influence genetic diversity of the two fragmented *T. camschatcense* populations in the Tokachi region. As a result, it was shown that genetic drift during reproduction causes significant diversity loss at seedlings especially in the small SAK population, and that stasis at 1L and 3L stages could buffer the stochasticity and maintain local genetic diversity in both populations. It should be noted that the comparison of two populations might be insufficient to draw general conclusions. However, considering that the two studied populations were representative in terms of FL density and habitat area (Figure 3), our discussion might be applicable to at least the other populations in the same region. While the need to facilitate reproduction and recruitment had been already highlighted from a demographic point of view (Ohara et al., 2006; Tomimatsu & Ohara, 2002; Tomimatsu & Ohara, 2004), this study, for the first time, revealed the importance of the survival of established individuals in terms of genetic diversity. Taken together, it is suggested that the whole life history processes should be considered for the conservation in fragmented *T. camschatcense* populations

in the Tokachi region.

Acknowledgements

We thank landowners, Obihiro City government, and Hiroo Town government for kindly allow our fieldwork. We are also grateful to T. Takada for his advice on our simulation analysis. This study was supported by Sasakawa Scientific Research Grant from the Japan Science Society (2019-5027) and Grants-in-Aid for Scientific Research from the Japan Society for the Promotion of Science (19H03294 and 20K06821).

References

Aguilar, R., Quesada, M., Ashworth, L., Herrerias-Diego, Y., & Lobo, J. (2008). Genetic consequences of habitat fragmentation in plant populations: susceptible signals in plant traits and methodological approaches. *Molecular Ecology, 17*, 5177-5188. doi: 10.1111/j.1365-294X.2008.03971.x

Aguilar, R., Calviño, A., Ashworth, L., Aguirre-Acosta, N., Carbone, L. M., Albrieu-Llinás, G., ... Cagnolo, L. (2018). Unprecedented plant species loss after a decade in fragmented subtropical Chaco Serrano forests. *Plos One, 13*, e0206738. doi: 10.1371/journal.pone.0206738

Aguilar, R., Cristóbal-Pérez, E. J., Balvino-Olvera, F. J., de Jesús Aguilar-Aguilar, M., Aguirre-Acosta, N., Ashworth, L., ... & Quesada, M. (2019). Habitat fragmentation reduces plant progeny quality: a global synthesis. *Ecology letters, 22*(7), 1163-1173. doi: 10.1111/ele.13272

534 Aldrich, P. R., Hamrick, J. L., Chavarriaga, P., & Kochert, G. (1998). Microsatellite
535 analysis of demographic genetic structure in fragmented populations of the tropical
536 tree *Symphonia globulifera*. *Molecular Ecology*, *7*, 933-944. doi: 10.1046/j.1365-
537 294x.1998.00396.x
538 Ally, D., & Ritland, K. (2006). A case study: looking at the effects of fragmentation on
539 genetic structure in different life history stages of old-growth mountain hemlock
540 (*Tsuga mertensiana*). *Journal of Heredity*, *98*, 73-78. doi: 10.1093/jhered/esl048
541 Aparicio, A., Hampe, A., Fernández-Carrillo, L., & Albaladejo, R. G. (2012).
542 Fragmentation and comparative genetic structure of four mediterranean woody
543 species: complex interactions between life history traits and the landscape context.
544 *Diversity and Distribution*, *18*, 226-235. doi: 10.1111/j.1472-4642.2011.00823.x
545 Bakker, J., van Rijswijk, M. E. C., Weissing, F. J., & Bijlsma, R. (2010). Consequences
546 of fragmentation for the ability to adapt to novel environments in experimental
547 *Drosophila* metapopulations. *Conservation Genetics*, *11*, 435-448. doi:
548 10.1007/s10592-010-0052-5
549 Borcard, D., Gillet, F., & Legendre, P. (2011). *Numerical Ecology with R*. New York:
550 Springer.
551 Bolger, A. M., Lohse, M., & Usadel, B. (2014). Trimmomatic: a flexible trimmer for
552 Illumina sequence data. *Bioinformatics*, *30*, 2114-2120. doi:
553 10.1093/bioinformatics/btu170
554 Caswell, H. (2001). *Matrix Population Models: Construction, Analysis, and*
555 *Interpretation*, 2nd edn. Sunderland: Sinauer Associates. Inc.
556 Coltman, D. W., Pilkington, J. G., Smith, J. A., & Pemberton, J. M. (1999). Parasite-
557 mediated selection against inbred Soay sheep in a free-living island populaton.

Evolution, *53*, 1259-1267. doi: 10.1111/j.1558-5646.1999.tb04538.x

Crow, J. F., & Morton, N. E. (1955). Measurement of gene frequency drift in small populations. *Evolution*, *9*, 202-214. doi: 10.2307/2405589

Ellner, S. (1996). Environmental fluctuations and the maintenance of genetic diversity in age or stage-structured populations. *Bulletin of Mathematical Biology*, *58*, 103-127. doi: 10.1016/0092-8240(95)00309-6

Ellner, S., & Hairston, N. G. Jr. (1994). Role of overlapping generations in maintaining genetic variation in a fluctuating environment. *American Naturalist, 143*, 403-417. doi: 10.1086/285610

González, A. V., Gómez-Silva, V., Ramírez, M. J., & Fontúrbel, F. E. (2020). Meta-analysis of the differential effects of habitat fragmentation and degradation on plant genetic diversity. *Conservation Biology*, *34*(5), 711-720. doi: 10.1111/cobi.13422

Goudet, J. (2005). HIERFSTAT, a package for R to compute and test hierarchical F-statistics. *Molecular Ecology Note*. *5*, 184-186. doi: 10.1111/j.1471-8278 .2004.00828.x

Hokkaido Government. (1897). *Hokkaido Shokuminchi Sentei Daini Houbun*. Sapporo: Hokkaido Government.

Hui, T. Y. J., & Burt, A. (2015). Estimating effective population size from temporally spaced samples with a novel, efficient maximum likelihood algorithm. *Genetics*, *200*, 285-293. doi: 10.1534/genetics.115.174904

Jombart, T. (2008). adegenet: a R package for the multivariate analysis of genetic markers. *Bioinformatics*, *24*, 1403-1405. doi: 10.1093/bioinformatics/btn129

Kramar, A. T., Ison, J. L., Ashley, M. V., & Howe, H. F. (2008). The paradox of forest fragmentation genetics. *Conservation Biology*, *22*(4), 878-885. doi: 10.1111/j.1523-

1739.2008.00944.x

Krauss, J., Bommarco, R., Guardiola, M., Heikkinen, R. K., Helm, A., Kuussaari, M., ... Steffan-Dewenter, I. (2010). Habitat fragmentation causes immediate and time-delayed biodiversity loss at different trophic levels. *Ecology Letters*, *13*, 597-605. doi: 10.1111/j.1461-0248.2010.01457.x

Lande, R. (1988). Genetics and demography in biological conservation. *Science, 241*, 1455-1460. doi: 10.1126/science.3420403

Leimu, R., Mutikainen, P., Koricheva, J., & Fischer, M. (2006). How general are positive relationships between plant population size, fitness and genetic variation? *Journal of Ecology*, *94*, 942-952. doi: 10.1111/j.1365-2745.2006.01150.x

Li, X. Y., Kurokawa, S., Giaimo, S., & Traulsen, A. (2016). How life history can sway the fixation probability of mutants. *Genetics*, *203*, 1297-1313. doi: 10.1534/genetics.116.188409

Lowe, A. J., Boshier, D., Ward, M., Bacles, C. F. E., & Navarro, C. (2005). Genetic resource impacts of habitat loss and degradation; reconciling empirical evidence and predicted theory for neotropical trees. *Heredity*, *95*, 255-273. doi: 10.1038/sj.hdy.6800725

Martins, E. M., Lamont, R. W., Martinelli, G., Lira-Medeiros, C. F., Quinet, A., & Shapcott, A. (2015). Genetic diversity and population genetic structure in three threatened *Ocotea* species (Lauraceae) from Brazil's Atlantic Rainforest and implications for their conservation. *Conservation Genetics*, *16*, 1-14. doi: 10.1007/s10592-014-0635-7

Murray, M. G., & Thompson, W. F. (1980). Rapid isolation of high molecular weight plant DNA. *Nucleic Acids Research, 8*, 4321-4326. doi: 10.1093/nar/8.19.4321

606 Nei, M., & Chesser, R. K. (1983). Estimation of fixation indices and gene diversities.
607 *Annals of Human Genetics*, *47*, 253-259. doi: 10.1111/j.1469-1809.1983.tb00993.x
608 Ohara, M., & Higashi, S. (1987). Interference by ground beetles with the dispersal by
609 ants of seeds of *Trillium* species (Liliaceae). *Journal of Ecology*, *75*, 1091-1098.
610 doi: 10.2307/2260316
611 Ohara, M., & Kawano, S. (2005). Life-history monographs of Japanese plants. 2:
612 *Trillium camschatcense* Ker-Gawl.(Trilliaceae). *Plant Species Biology*, *20*, 75-82.
613 doi: 10.1111/j.1442-1984.2005.00126.x
614 Ohara, M., Takeda, H., Ohno, Y., & Shimamoto, Y. (1996). Variations in the breeding
615 system and the population genetic structure of *Trillium kamtschaticum* (Liliaceae).
616 *Heredity*, *76*, 476-484. doi: 10.1038/hdy.1996.70
617 Ohara, M., Tomimatsu, H., Takada, T., & Kawano, S. (2006). Importance of life history
618 studies for conservation of fragmented populations: a case study of the understory
619 herb, *Trillium camschatcense*. *Plant Species Biology*, *21*, 1-12. doi: 10.1111/j.1442-
620 1984.2006.00145.x
621 Oksanen, J., Blanchet, F. G., Friendly, M., Kindt, R., Legendre, P., McGlinn, D., ...
622 Wagner, H. (2019). vegan: community ecology package. R package version 2.5-3.
623 Retrieved from https://CRAN.R-project.org/package=vegan
624 Ramsayer, J., Kaltz, O., & Hochberg, M. E. (2012). Evolutionary rescue in populations
625 of *Pseudomonas fluorescens* across an antibiotic gradient. *Evolutionary*
626 *Applications*, *6*, 608-616. doi: 10.1111/eva.12046
627 Reed, D. H., & Frankham, R. (2003). Correlation between fitness and genetic diversity.
628 *Conservation Biology*, *17*(1), 230-237. doi: 10.1046/j.1523-1739.2003.01236.x
629 Rochette, N. C., Rivera-Colón, A. G., & Catchen, J. M. (2019). Stacks 2: Analytical

methods for paired-end sequencing improve RADseq-based population genomics. *Molecular Ecology*, *28*, 4737-4754. doi: 10.1111/mec.15253

Silvertown, J., Franco, M., Pisanty, I., & Mandoza, A. (1993). Comparative plant demography – relative importance of life-cycle components to the finite rate of increase in woody and herbaceous perennials. *Journal of Ecology*, *81*, 465-476. doi: 10.2307/2261525

Stoffel, M. A., Esser, M., Kardos, M., Humble, E., Nichols, H., David, P., & Hoffman, J. I. (2016). inbreedR: an R package for the analysis of inbreeding based on genetic markers. *Methods in Ecology and Evolution*, *7*, 1331-1339. doi: 10.1111/2041-210X.12588

Suyama, Y., & Matsuki, Y. (2015). MIG-seq: an effective PCR-based method for genome-wide single-nucleotide polymorphism genotyping using the next-generation sequencing platform. *Scientific Reports*, *5*, 16963. doi: 10.1038/srep16963

Takada, T., & Kawai, Y. (2020). An analysis of elasticity vector distribution specific to semelparous species using randomly generated population projection matrices and the COMPADRE Plant Matrix Database. *Ecological Modelling*, *431*, 109125. doi: 10.1016/j.ecolmodel.2020.109125

Toczydlowski, R. H., & Waller, D. M. (2019). Drift happens: Molecular genetic diversity and differentiation among populations of jewelweed (*Impatiens capensis* Meerb.) reflect fragmentation of floodplain forests. *Molecular Ecology*, *28*, 2459-2475. doi: 10.1111/mec.15072

Tomimatsu, H., & Ohara, M. (2002). Effects of forest fragmentation on seed production of the understory herb *Trillium camschatcense*. *Conservation Biology*, *16*, 1277-1285. doi: 10.1046/j.1523-1739.2002.00412.x

654 Tomimatsu, H., & Ohara, M. (2003). Genetic diversity and local population structure of
655 fragmented populations of *Trillium camschatcense* (Trilliaceae). *Biological*
656 *Conservation*, *109*, 249-258. doi: 10.1016/S0006-3207(02)00153-2
657 Tomimatsu, H., & Ohara, M. (2004). Edge effects on recruitment of *Trillium*
658 *camschatcense* in small forest fragments. *Biological Conservation, 117*, 509-519.
659 doi: 10.1016/j.biocon.2003.08.010
660 Tomimatsu, H., & Ohara, M. (2006). Evaluating the consequences of habitat
661 fragmentation: a case study in the common forest herb *Trillium camschatcense*.
662 *Population Ecology*, *48*, 189-198. doi: 10.1007/s10144-006-0269-9
663 Tomimatsu, H., & Ohara, M. (2010). Demographic response of plant populations to
664 habitat fragmentation and temporal environmental variability. *Oecologia*, *162*, 903-
665 911. doi: 10.1007/s00442-009-1505-8
666 Waples, R. S., & Teel, D. J. (1990). Conservation genetics of Pacific salmon I. temporal
667 changes in allele frequency. *Conservation Biology*, *4*, 144-156. doi: 10.1111/j.1523-
668 1739.1990.tb00103.x
669 Williams, S. L. (2001). Reduced genetic diversity in eelgrass transplantations affects
670 both population growth and individual fitness. *Ecological Applications, 11*(5), 1472-
671 1488. doi: 10.1890/1051-0761(2001)011[1472:RGDIET]2.0.CO;2
672 Young, A., Boyle, T., & Brown, T. (1996). The population genetic consequences of
673 habitat fragmentation for plants. *Trends in Ecology and Evolution, 11*, 413-418. doi:
674 10.1016/0169-5347(96)10045-8
675
676
677

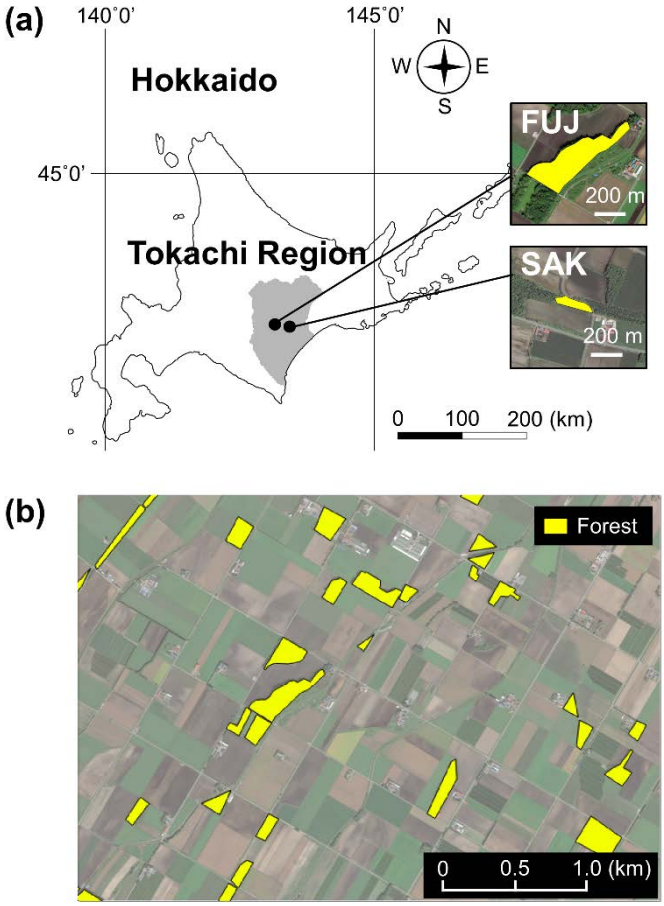

678

679 **Figure 1.** (a) The location of the Tokachi region and the two studied populations: SAK

680 (Sakuragi, small population) and FUJ (Fuji, large population). (b) An iconic aerial view

681 of fragmented forests in the Tokachi region

682

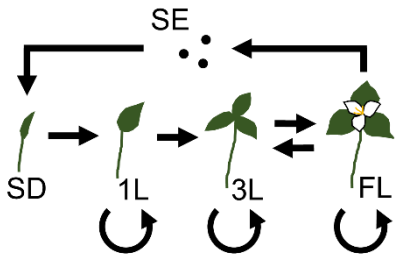

683

684 **Figure 2.** Life history of *Trillium camschatcense*. Arrows represent the possible annual

685 trajectory of individuals. SE, seed; SD, seedling; 1L, one-leaf; 3L, three-leaves; FL,

686 flowering

687

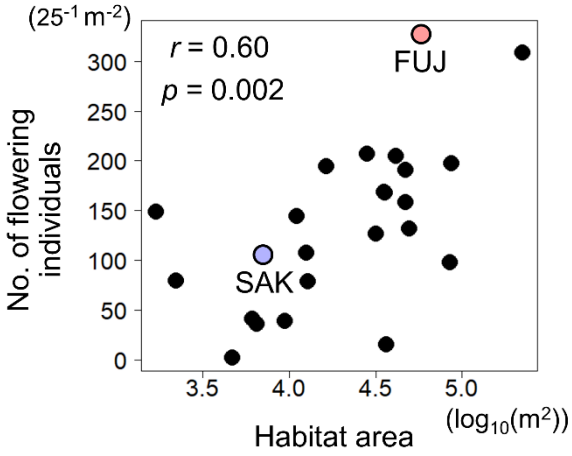

688

689 **Figure 3.** A positive effect of habitat area on the density of flowering individuals

690 revealed by preliminary survey in 2018. Blue and red circles represent the data of SAK

691 (Sakuragi) and FUJ (Fuji) population, respectively

692

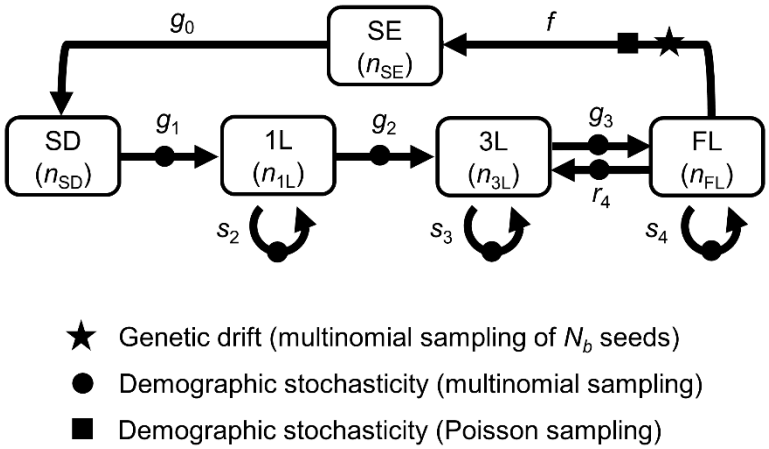

693

694 **Figure 4.** Population updating rules used in simulation analyses. g_0 is germination rate
695 of SE (seed). g_1, g_2, and g_3 are the growth rates of SD (seedling), 1L (one-leaf), and 3L
696 (three-leaves). s_2, s_3, and s_4 are the stasis rates of 1L, 3L, and FL (flowering). r_4 and f
697 are the retrogression rate and fecundity of FL. At each timestep (year), the fate of
698 individuals was determined depending on these demographic rates. When incorporating
699 genetic drift (scenario 2 and 4), we did multinomial sampling N_b times to determine the
700 genotype frequencies of SE (seed), as marked with star symbol. When incorporating
701 demographic stochasticity (scenario 3 and 4), we applied multinomial and Poisson
702 sampling at transitions marked with circle and square, respectively. The number of
703 individuals were kept constant (SE, n_{SE}; SD, n_{SD}; 1L, n_{1L}; 3L, n_{3L}; FL, n_{FL}) by scaling
704 at each time step
705

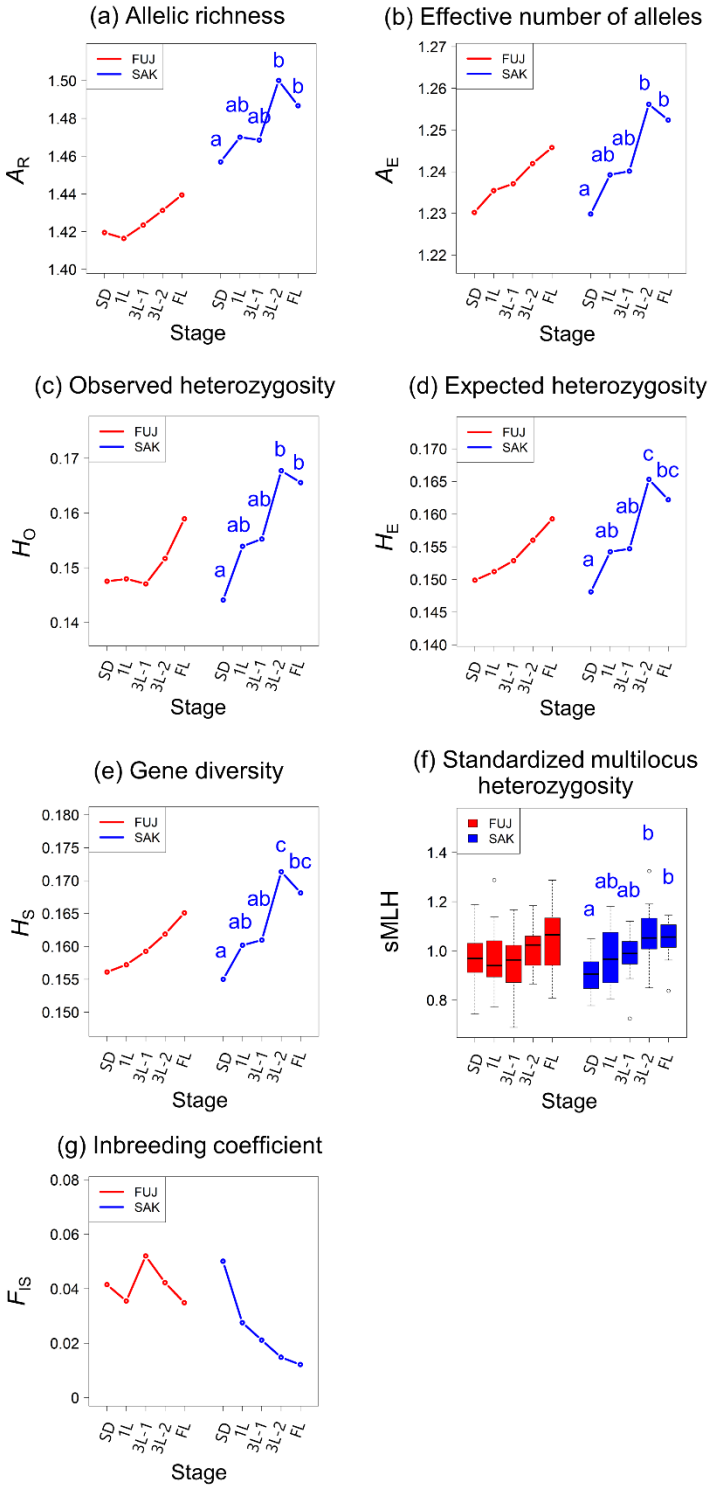

706

707 **Figure 5.** (a) Allelic richness A_R, (b) effective number of alleles A_E, (c) observed

708 heterozygosity H_O, (d) expected heterozygosity H_E, (e) gene diversity H_S, (f)

709 standardized multilocus heterozygosity sMLH, and (g) inbreeding coefficient F_{IS} at each

life history stage (SE (seed), SD (seedling), 1L (one-leaf), 3L (three-leaves), and FL (flowering)) of both populations. Data shown in red and blue are that of FUJ (Fuji, large population) and SAK (Sakuragi, small population), respectively. sMLH, which was estimated per individual, are shown in box plot, while the other indices estimated per stage are shown in dots. Significant difference was detected by permutation test for pairs marked with different alphabets (significance level = 0.05). No alphabet signs are assigned when there were no statistically significant differences

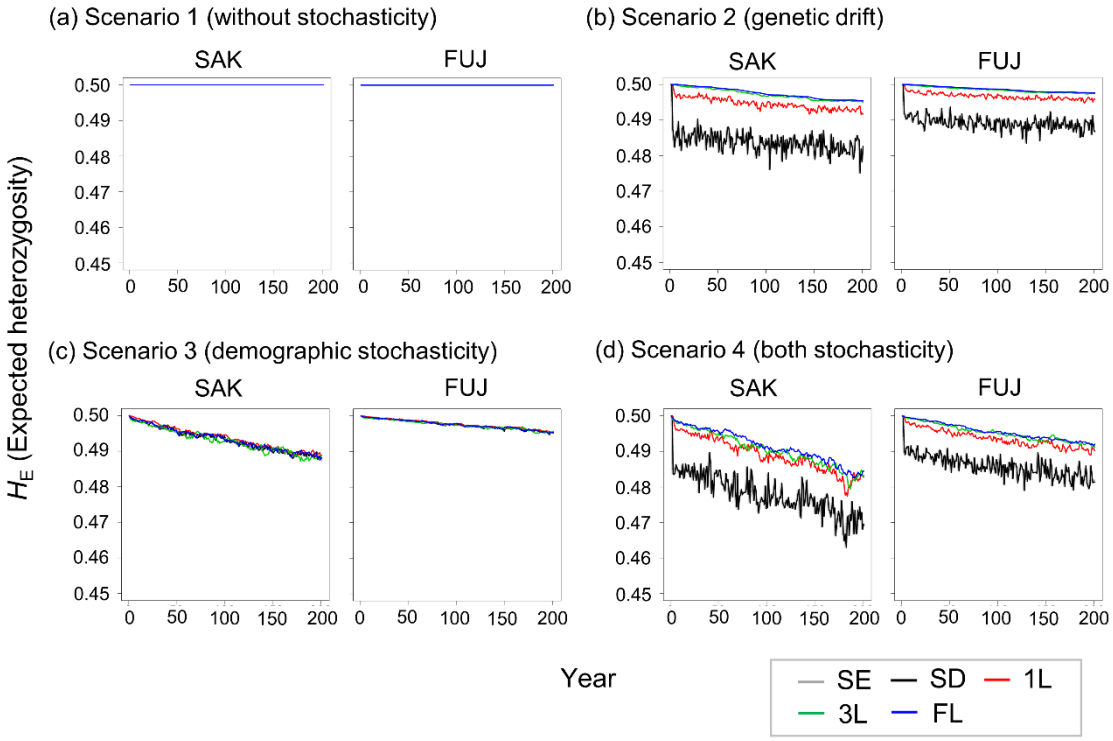

Figure 6. Temporal changes in expected heterozygosity (H_E) of the five stages (SE (seed), SD (seedling), 1L (one-leaf), 3L (three-leaves), and FL (flowering)) in SAK (Sakuragi, small population) and FUJ (Fuji, large population) under the four scenarios: no stochasticity (scenario 1), genetic drift (scenario 2), demographic stochasticity (scenario 3), and both genetic drift and demographic stochasticity (scenario 4)

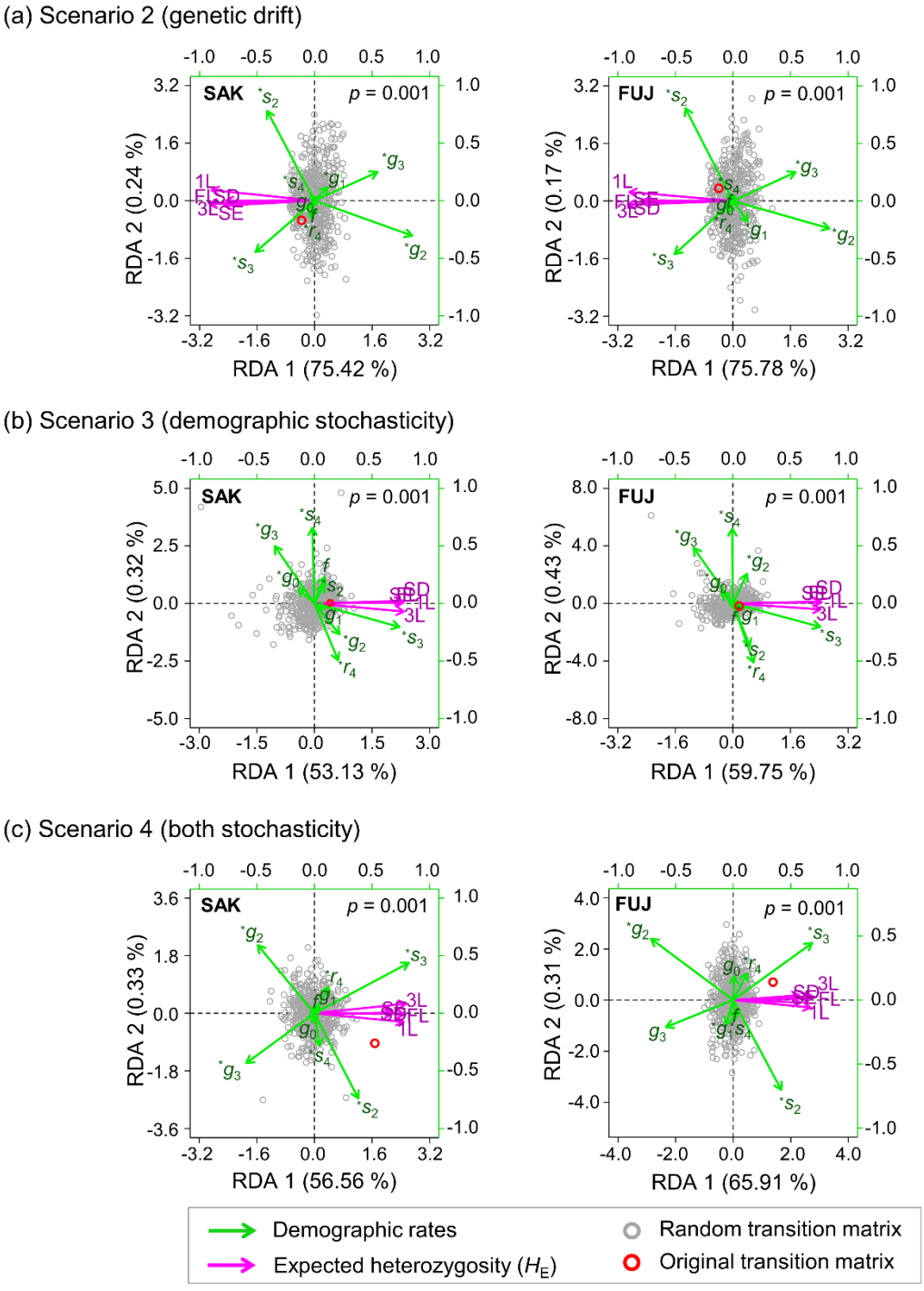

Figure 7. RDA correlation triplots of SAK (Sakuragi, small population) and FUJ (Fuji, large population) under genetic drift (scenario 2), demographic stochasticity (scenario 3), and both (scenario 4). Top and right-hand axes are for constraints (demographic rates), while bottom and left-hand axes are for H_E of the five stages (SE (seed), SD (seedling),

730 1L (one-leaf), 3L (three-leaves), and FL (flowering)) and ordinated 501 trials. For each
731 panel, the angles among arrows reflect their correlations: those in the same direction have
732 positive correlations, while those in the opposite direction have negative correlations. *P*
733 values of the overall ordination were shown at the topright margin of each figure. *
734 denotes constraint variables significantly constituting the ordination (significance level =
735 0.05). Percentages presented in axis labels indicate the explanatory power of the axes